Formation of Nitric Oxide Synthase−Iron(II) Nitrosoalkane Complexes: Severe Restriction of Access to the Iron(II) Site in the Presence of Tetrahydrobiopterin

Axelle Renodon,[‡] Jean-Luc Boucher,[‡] Chaoqun Wu,[§] Ratan Gachhui,[§] Marie-Agnès Sari,[‡] Daniel Mansuy,*[,‡] and Dennis Stuehr[§]

Laboratoire de Chimie et Biochimie Pharmacologiques et Toxicologiques, URA 400 CNRS, Université Paris V, 45 Rue des Saints-Pères, 75270 Paris Cedex 06, France, and Department of Immunology, The Cleveland Clinic Foundation, 9500 Euclid Avenue, Cleveland, Ohio 44195

Received September 15, 1997; Revised Manuscript Received December 16, 1997

ABSTRACT: Nitric oxide synthases (NOS) are heme proteins, closely related to cytochromes P450, that catalyze oxidation of L-arginine (L-Arg) to nitric oxide (NO) and citrulline. To get further insight into their active site, we have studied the ability of recombinant mouse inducible NOS (iNOS) and rat brain neuronal NOS (nNOS), and of their oxygenase domains ($iNOS_{oxy}$ and $nNOS_{oxy}$), to form Fe(II)−nitrosoalkane complexes. In the absence of BH_4, $iNOS_{oxy}$, $nNOS_{oxy}$, and full-length iNOS readily form complexes characterized by Soret peaks around 448 nm, after reaction with various nitroalkanes and sodium dithionite. These complexes displayed physicochemical characteristics very similar to those of previously reported microsomal cytochrome P450−Fe(II)−nitrosoalkane complexes: (i) a Soret peak around 450 nm, (ii) a clear stability in the presence of CO, and (iii) a fast destruction upon oxidation of the iron by ferricyanide. Thus, in the absence of L-Arg and BH_4, NOSs Fe(II) appear to be largely opened to even large R−NO ligands with R = cyclohexyl or *p*-Cl−C_6H_4−$CH_2CH(CH_3)$ for instance, in a manner similar to microsomal P450s Fe(II). As expected, the presence of L-Arg inhibits the formation of NOSs Fe(II)−RNO complexes. More surprisingly, the presence of BH_4 also strongly inhibits the formation of the NOSs Fe(II) complexes even with the smallest nitrosoalkane ligand, CH_3NO (IC_{50} values of 0.5 and 4 μM for $nNOS_{oxy}$ and $iNOS_{oxy}$, respectively). Accordingly, recombinant full-length nNOS containing BH_4 and L-Arg is completely unable to form Fe(II)−nitrosoalkane complexes, even with CH_3NO. These results suggest that, in the absence of L-Arg and BH_4, the distal pocket of NOSs Fe(II) is largely opened even to bulky ligands, in a manner similar to that of microsomal cytochromes P450. On the contrary, the distal heme pocket of iNOS and nNOS seems to be closed after binding of L-Arg and BH_4, particularly in the Fe(II) state. This results in a highly restricted access for Fe(II) ligands, except very small ones such as CO, NO, and O_2. Such effects of BH_4 in controlling the size of the distal heme pocket of NOS Fe(II) correspond to a new role of biopterins in biological systems.

Nitric oxide (NO)[1] plays important roles in the physiology of many organisms, including man (*1*, *2*). NO is generated from L-arginine in a NADPH-dependent stepwise oxidation that is catalyzed by NO synthases (NOSs) (*3*, *4*). Three distinct NOS isoforms have been cloned from several sources, including neurons, endothelial cells, and macrophages. Neuronal and endothelial NOSs are constitutively expressed in an inactive form and require Ca^{2+}-dependent calmodulin (CaM) binding to activate their NO synthesis. In contrast, expression of macrophage NOS is only observed following induction by immunoactive cytokines such as interferon-γ or interleukin 2. Once expressed, macrophage NOS continuously generates NO in a Ca^{2+}-independent manner due to its containing CaM as a tightly bound prosthetic group (*3*, *5*).

Despite their differences in expression and CaM binding, the constitutive and inducible NOSs contain the same prosthetic groups, and their basic structural organization appears to be conserved. The COOH terminal domain binds NADPH and the two flavins FAD- and FMN; it exhibits a high sequence similarity with other FAD and FMN-dependent reductases that transfer electrons to heme proteins, including NADPH cytochrome P450 reductase (*6*). The basic, hydrophobic central peptide appears to be responsible for calmodulin binding (*7*). The NH_2 terminal domain binds tetrahydrobiopterin (BH_4), iron−protoporphyrin IX (heme), and L-arginine, and by itself it can homodimerize. Recent studies have shown that heme, L-arginine, and BH_4 are all required to form active dimeric NOSs from catalytically inactive monomers (*8*−*14*).

The NOS oxygenase domain exhibits some characteristics in common with cytochromes P450 (*5*, *15*−*18*). Its heme

* To whom correspondence should be addressed. Fax: 33 01 42 86 83 87.

‡ Université Paris V.

§ The Cleveland Clinic Foundation.

[1] Abbreviations: L-Arg, L-arginine; CaM, calmodulin; BH_4, (*6R*)-5,6,7,8-tetrahydro-L-biopterin; (*6S*)-BH_4, (*6S*)-5,6,7,8-tetrahydro-L-biopterin; BH_2, 7,8-dihydro-L-biopterin; 6,7-diMe-TP, 6,7-dimethyl-5,6,7,8-tetrahydropterin; HEPES, 4-(2-hydroxyethyl)-1-piperazineethanesulfonic acid; NO, nitric oxide; NOS, nitric oxide synthase; $iNOS_{oxy}$, inducible NO synthase, oxygenase domain; $nNOS_{oxy}$, neuronal NO synthase, oxygenase domain.

S0006-2960(97)02297-6 CCC: $15.00
Published on Web 04/15/1998

iron is bound to the protein through a cysteinate proximal ligand, and its iron(III) resting state exists as a mixture of a low-spin hexacoordinate complex and a high-spin pentacoordinate complex in equilibrium. Addition of L-arginine shifts this equilibrium toward the pentacoordinate species (*19*). However, the nature of the distal environment of the heme in NOSs and the coordination chemistry of these enzymes remain poorly known. In fact, only a few iron(III) or iron(II) complexes of NOSs have been reported so far. NOS−iron(III) complexes with cyanide (*20*), various nitrogen-containing ligands (*19*, *21*, *22*), and NO (*23*−*25*) have been described. Moreover, the formation of σ-aryl−iron complexes of the NOSs has been reported recently (*26*, *27*). In the case of NOS−iron(II), only complexes with very small ligands such as CO (*15*), NO (*24*), and O_2 (*28*) are known.

In an effort to better know the distal environment and coordination chemistry of the heme in NOS−Fe(II) as a function of the presence of BH_4 and L-arginine, and to compare this environment to that of cytochromes P450, we tried to prepare a series of NOS−Fe(II) complexes with more or less bulky ligands. The heme proteins used in this study were recombinant NOS-based proteins, iNOS and nNOS or their oxygenase domains, that have been expressed in *Escherichia coli* or yeast and purified with or without BH_4. The ligands used in this study were nitrosoalkanes, RNO, that are isoelectronic with O_2 and form strong bonds with iron(II) heme proteins as they involve a low-lying π^* system readily available for back-bonding (*29*). Tertiary nitrosoalkanes, such as $(CH_3)_3CNO$, are too bulky to bind to iron(II)porphyrins and heme proteins, whereas primary and secondary nitrosoalkanes, R_1R_2CHNO, readily bind to iron(II)porphyrins (*29*). It is noteworthy that those nitrosoalkanes, R_1R_2CHNO, are unstable by themselves because of their fast isomerization to the corresponding oximes $R_1R_2C{=}NOH$. Therefore, the only way to prepare iron(II)−$N(O)CHR_1R_2$ complexes is to generate the nitrosoalkanes in situ in the vicinity of the iron(II) center, by a proper chemical transformation of stable precursors, either nitroalkanes $R_1R_2CHNO_2$ or hydroxylamines, $R_1R_2CHNHOH$. Thus, very stable iron(II)−nitrosoalkane complexes of hemoglobin, myoglobin (*30*), cytochrome P450 (*31*, *32*), and cyclooxygenase (*33*) have been obtained upon reaction of these heme proteins, either with the corresponding hydroxylamines, $R_1R_2CHNHOH$, under oxidizing conditions, or with the corresponding nitroalkanes, $R_1R_2CHNO_2$, in the presence of a reducing agent (eqs 1 and 2).

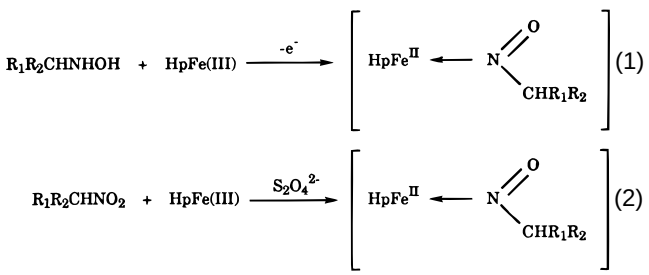

Formation of such complexes with relatively bulky nitrosoalkane ligands depends on the size of the heme protein distal pocket. For instance, hemoglobin or myoglobin, which have a restricted access to the heme, only accommodate relatively small nitrosoalkane ligands (with $R_1 = R_2 = H$; $R_1 = H$, $R_2 = CH_3$; and $R_1 = R_2 = CH_3$), whereas liver microsomal cytochromes P450, such as CYP 3A4, may bind very large nitrosoalkane ligands, including that derived from the macrolide antibiotic troleandomycin (*34*).

This paper shows that, in the absence of BH_4 and L-arginine, the oxygenase domains of iNOS and nNOS, as well as full-length iNOS, readily form iron(II)−nitrosoalkane complexes upon reaction of various nitroalkanes and dithionite. However, the formation of these iron(II)−nitrosoalkane complexes is strongly inhibited in the presence of BH_4, and recombinant nNOS containing BH_4 is unable to form such complexes.

MATERIALS AND METHODS

Chemicals. Nitromethane, nitroethane, 2-nitropropane (isopropyl-NO_2), 2-methyl-2-nitropropane (*tert*-butyl-NO_2), 1-nitrohexane, nitrocyclohexane, and nitrobenzene were purchased from Janssen. Sodium dithionite was purchased from Merck, and L-arginine and potassium ferricyanide were from Sigma. (*6R*)-5,6,7,8-Tetrahydro-L-biopterin dihydrochloride (BH_4), (*6S*)-5,6,7,8-tetrahydro-L-biopterin [(*6S*)-BH_4], 7,8-dihydro-L-biopterin dihydrochloride (BH_2), and 6,7-dimethyl-5,6,7,8-tetrahydropterin hydrochloride (6,7-diMe-TP) came from Alexis Co. 1-(4-Chlorophenyl)-1-nitroethane was obtained after bromination of 1-(4-chlorophenyl)ethanol (Janssen) by PBr_3 in pyridine, followed by reaction with sodium nitrite in anhydrous DMSO according to previously described procedures (*35*). Condensation of 4-chlorobenzaldehyde (Janssen) with nitroethane gave 1-(4-chlorophenyl)-2-nitropropene (*36*), which was thus reduced by $NaBH_4$ to 1-(4-chlorophenyl)-2-nitropropane following a described procedure (*37*). All other chemicals were obtained from sources as indicated in the text and were of the highest quality commercially available.

Protein Expression and Purification. (A) Full-Length Inducible Nitric Oxide Synthase. Recombinant full-length dimeric inducible NOS was isolated and purified from *E. coli* as described previously (*38*). *E. coli* was transformed with a plasmid containing mouse iNOS with a six-histidine tag on its N-terminus, and a plasmid that contained human calmodulin. Coexpression with calmodulin enabled production of active full-length iNOS, which could be recovered in pure form by binding it to nickel affinity resin (Ni−Nitrilotriacetate TSepharose CL4B resin, Pharmacia Biotech, Inc.), washing the resin to remove unbound proteins, and eluting with imidazole according to the manufacturer's directions. Eluted protein was concentrated and subjected to 2′,5′-ADP affinity chromatography as described (*39*).

(B) Full-Length Neuronal Nitric Oxide Synthase. Full-length neuronal NOS was overexpressed in *Saccharomyces cerevisiae* stably transfected with the A 379 plasmid carrying the rat brain NOS cDNA (*39*). The culture procedures used to achieve nNOS expression in yeast were identical to those described previously for the inducible NOS (*40*), and neuronal NOS was isolated and purified by binding it to calmodulin affinity resin (Calmodulin Agarose column, Sigma Chemicals Co.) as described previously (*39*).

(C) Oxygenase Domains of Inducible and Neuronal Nitric Oxide Synthases. The iNOS oxygenase domain (amino acids 1−498) and the nNOS oxygenase domain (amino acids

1−723) containing a six-histidine tag at their C terminus were overexpressed in *E. coli* strain BL21(DE3) using a modified version of the PCW*ori* vector, which has been used to express the oxygenase domain of neuronal NOS (*41*). The oxygenase domains were isolated by binding to nickel affinity resin (Ni−Nitrilotriacetate TSepharose CL4B resin, Pharmacia Biotech Inc.), washing the resin, and eluting with imidazole according to the manufacturer's directions. Characterization of the domains (*12*, *28*, *42*, *43*) showed that they were dimeric and had the same spectral and binding properties as the native oxygenase domains that are formed by trypsinolysis of full-length dimeric NOSs (*41*). Purified oxygenase domain dimers were dialyzed against 40 mM 4-(2-hydroxyethyl)-1-piperazineethanesulfonic acid (HEPES), pH 7.6, containing 10% glycerol and 0.5 mM dithiothreitol prior to use. Oxygenase domain dimers were dissociated using 5 M urea (*42*, *43*). The dissociation reaction was carried out at 28 °C for 90 min and was terminated by a 10-fold dilution with 40 mM HEPES buffer, pH 7.6, containing 10% glycerol. The monomers so prepared were checked by gel filtration chromatography on Superdex 200.

Spectral Measurements. Spectra were recorded at room temperature (20 °C) on a Kontron 942 spectrophotometer. Enzyme concentrations are reported on a per heme basis and were determined from the absorbance difference between 444 and 490 nm for the dithionite-reduced CO-bound NOS, using an estimated extinction coefficient of 72 mM^{-1} cm^{-1} (*16*). Enzyme (usually 0.5−1.0 μM, in 150 μL 50 mM HEPES buffer, pH 7.4) was added either to the reference cuvette only (absolute spectra) or to both cuvettes (differential mode). The studied compounds were introduced to the sample cuvette dissolved in buffer (or in DMSO for 1-nitrohexane and nitrocyclohexane; maximal solvent volume was less than 1%), and a similar volume of buffer (or DMSO) was added to the reference cuvette. Sodium dithionite was added to both cuvettes just before scanning between 370 and 500 nm at a 200 nm/min rate. In some cases, the enzyme was preincubated for 10 min at room temperature with L-arginine, BH_4, or other compounds dissolved in 50 mM HEPES buffer, pH 7.4.

RESULTS

Reaction of Nitromethane with the iNOS Dimeric Oxygenase Domain (iNOS$_{oxy}$) in the Presence of Dithionite. Recombinant murine $iNOS_{oxy}$ has been produced in *E. coli* and purified in the absence of BH_4 and L-Arg; it exists primarily (∼80%) under a dimeric form (*43*). In the presence of sodium dithionite, it showed an UV−visible spectrum typical for $iNOS_{oxy}$ Fe(II) with a Soret peak at 413 nm (Figure 1). Further addition of nitromethane led to the gradual appearance of a new spectrum with peaks at 448 and 548 nm as a function of time. When using 8 μM $iNOS_{oxy}$ and 2.5 mM nitromethane, maximal intensity of the spectrum was observed after 3 min and remained stable for more than 10 min. In fact, the intensity of the 448-nm peak only slowly decreased after 15 min (0.2%/min). Similar experiments were followed by difference spectroscopy using two cuvettes containing 1.2 μM $iNOS_{oxy}$. A typical difference spectrum obtained after reaction with nitromethane and dithionite is shown in Figure 2; it is characterized by a peak at 448 nm and a trough at 412 nm corresponding to the disappearance of $iNOS_{oxy}$−Fe(II). The maximum absorbance, ΔA (448−490 nm), observed for the complex derived from 1.2 μM $iNOS_{oxy}$, 2.5 mM nitromethane, and excess dithionite was similar to that obtained for the $iNOS_{oxy}$−Fe(II)−CO complex (ΔA 444−490 nm). This suggests an almost complete conversion of $iNOS_{oxy}$ to the new 448 nm absorbing complex under these conditions. When identical experiments were done by using 250 μM nitromethane, the 448-nm absorbing complex was formed more slowly and its maximal intensity was about 80% of that observed with 2.5 mM nitromethane. The 448 nm peak was also clearly observed when using a nitromethane concentration as low as 25 μM.

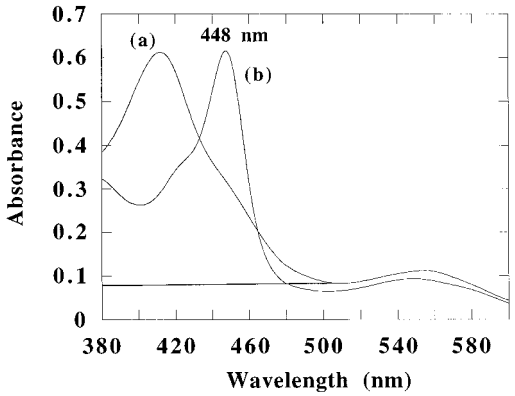

FIGURE 1: UV−Visible spectrum of the complex formed upon reaction of $iNOS_{oxy}$ with CH_3NO_2 in the presence of dithionite. (a) $iNOS_{oxy}$, 8 μM, in 50 mM HEPES buffer, pH 7.4, reduced by an excess of sodium dithionite. (b) Spectrum obtained 5 min after addition of 2.5 mM CH_3NO_2.

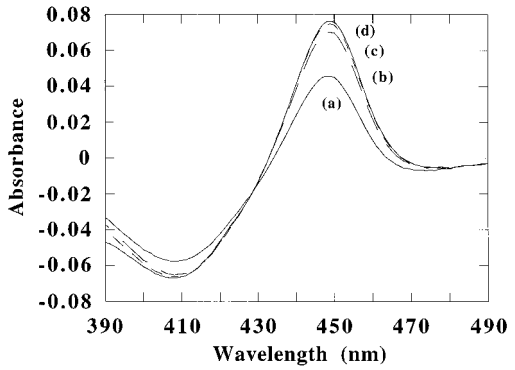

FIGURE 2: Difference spectra obtained upon reaction of $iNOS_{oxy}$ with CH_3NO_2 and dithionite as a function of time. The two cuvettes contained 1.2 μM $iNOS_{oxy}$ in 50 mM HEPES buffer, pH 7.4, reduced by an excess of dithionite (10 mM). CH_3NO_2, 2.5 mM, was then added to the sample cuvette, and the spectra were recorded every minute: curves a, b, c, and d correspond to 1, 2, 3, and 5 min.

The 448 nm absorbing complex remained stable for at least 15 min under aerobic conditions even after complete consumption of dithionite as shown by the disappearance of dithionite absorption around 350 nm. This complex remained stable after bubbling CO in the cuvette, as one did not observe any shift of the Soret peak toward 444 nm (data not shown). Finally, the only method to destroy this complex and to recover $iNOS_{oxy}$ in its ferric resting state was to add increasing amounts of the oxidant ferricyanide. Addition of 2 mM ferricyanide led to a complete disappearance of the 448-nm peak and its replacement with a 418-nm peak that is characteristic of low-spin $iNOS_{oxy}$−iron(III) (Figure 3).

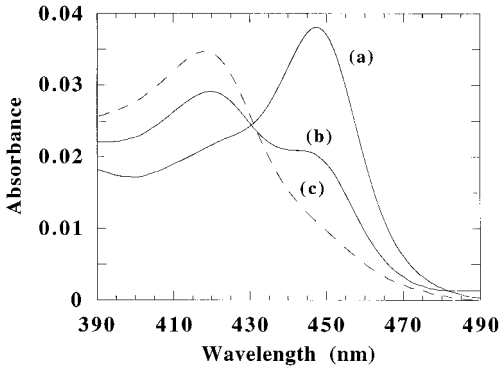

FIGURE 3: Destruction of the CH_3NO_2-derived 448 nm absorbing $iNOS_{oxy}$ complex by ferricyanide. (a) Absolute visible spectrum of the complex formed upon reaction of 0.6 μM $iNOS_{oxy}$ with 2.5 mM CH_3NO_2 and excess dithionite. (b) Addition of 1 mM potassium ferricyanide. (c) Further addition of 1 mM ferricyanide.

Thus, the 448 nm absorbing complex exhibits characteristics strikingly similar to those of the previously reported microsomal cytochrome P450−Fe(II)−N(O)CH_3 complex (*31*): (i) both complexes exhibit a Soret peak slightly redshifted when compared to the corresponding iron(II)−CO complexes (448 instead of 444 nm for $iNOS_{oxy}$ compared to 455 instead of 450 nm for cytochrome P450), (ii) both complexes are very stable even in the presence of a reducing agent in excess and do not exchange their ligand with CO, and (iii) both complexes are destroyed by ferricyanide giving back the starting ferric heme protein. This is in agreement with the properties previously found for porphyrin−Fe(II)−N(O)R (*29*) and heme protein−Fe(II)−N(O)R complexes (*34*), which exhibit a very strong, almost irreversible Fe(II)−N(O)R bond, but which, upon oxidation of the iron, for instance by ferricyanide, lead to highly unstable Fe(III)−N(O)R complexes that readily lose their nitrosoalkane ligand.

All these resemblances between the 448 nm absorbing $iNOS_{oxy}$ complex and cytochrome P450−Fe(II)−N(O)CH_3 strongly suggest that the former complex derives from the binding of nitrosomethane, CH_3NO, formed in situ by reduction of nitromethane, CH_3NO_2, to $iNOS_{oxy}$ Fe(II) in trans position relative to the proximal cysteinate ligand.

Reaction of Various Nitroalkanes with $iNOS_{oxy}$. Various nitroalkanes were found able to react with $iNOS_{oxy}$ in the presence of excess dithionite with formation of complexes exhibiting spectral properties similar to those derived from nitromethane. Only small variations of the Soret peak position of these complexes (λ_{max} = 450 ± 2 nm) were observed (Table 1). However, their rates of formation varied as a function of the nitroalkane structure (Figure 4 A and Table 1). The complexes derived from the smallest nitroalkanes (R = methyl and ethyl) were formed rapidly and almost completely within 3 min, whereas those derived from bigger nitroalkanes (R = isopropyl) were completely formed only after 10 min. Those derived from even more bulky or more hydrophobic substrates (R = cyclohexyl for instance) corresponded to an only partial transformation of $iNOS_{oxy}$ (as shown by their lower ΔA_{max}, Figure 4A). Finally, *tert*-butyl-NO_2 and nitrobenzene, Ph-NO_2, failed to give any complex under identical conditions (Table 1). This result is in agreement with what has been described for other heme proteins, as *tert*-butyl-NO is too bulky to bind to iron(II)-porphyrins, and as Fe(II)−N(O)Ph complexes that could have derived from Ph-NO_2 reduction are not stable in the presence of excess dithionite (*44*).

Table 1: Formation of Nitrosoalkane Complexes of $iNOS_{oxy}$ and $nNOS_{oxy}$ after Reaction with Nitroalkanes (R−NO_2) and Dithionite

	R	λ_{max}[a]	$iNOS_{oxy}$[b]	$nNOS_{oxy}$[c]
1	methyl	448	0.72	0.40
2	ethyl	449	0.54	0.41
3	isopropyl	450	0.32	0.15
4	*tert*-butyl	no peak		
5	4-Cl−Ph-$CHCH_3$[d]	448	0.06	n.d.[e]
6	4-Cl−Ph-CH_2CHCH_3[d]	451	0.10	n.d.[e]
7	hexyl	452	0.18	0.09
8	cyclohexyl	450	0.10	0.04
9	phenyl	no peak		

[a] Values for λ_{max} are in nanometers. Identical values were found for i- and $nNOS_{oxy}$ for each R−NO_2. [b] Initial rate of complex formation between 0.6 μM $iNOS_{oxy}$ and 2.5 mM nitroalkane in the presence of 10 mM sodium dithionite, expressed in nanomoles of complex (nmol of NOS^{-1}) min^{-1}. Calculations used an ϵ value identical for all complexes (45 ± 4.5 mM^{-1} cm^{-1}) assuming 100% complex formation in the case of CH_3NO_2. [c] As in footnote b, but with 0.4 μM $nNOS_{oxy}$. [d] Due to limited solubilities of these two compounds, the final concentration was 1 mM. [e] Not determined.

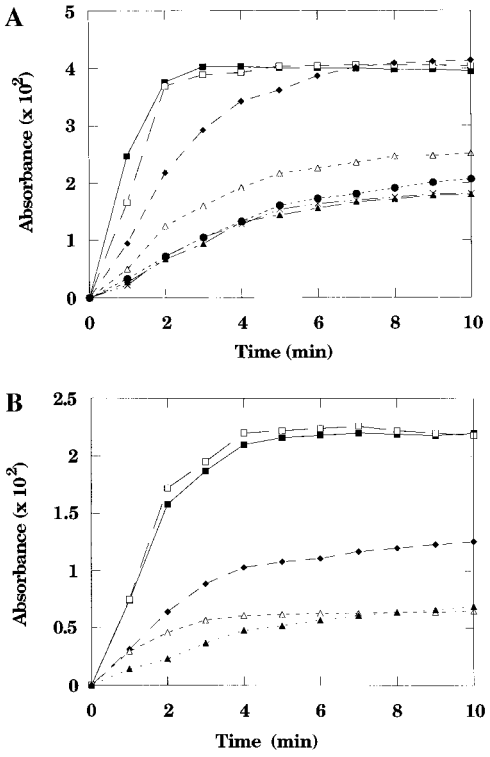

FIGURE 4: Kinetics of formation of nitrosoalkane complexes of $iNOS_{oxy}$ and $nNOS_{oxy}$ from *in situ* reduction of nitroalkanes. (A) ΔA (λ_{max}, 480 nm) of a 0.5 μM $iNOS_{oxy}$ solution was followed, as a function of time, after addition of 10 mM dithionite and 2.5 mM nitroalkane. ■, nitromethane; □, nitroethane; ◆, 2-nitropropane; △, 1-nitrohexane; ▲, nitrocyclohexane; ×, 1-(4-chlorophenyl)-1-nitroethane; ●, 1-(4-chlorophenyl)-2-nitropropane. Concentration of the last two compounds was 1 mM. (B) Identical experiments performed with 0.35 μM $nNOS_{oxy}$. Experiments using 1-(4-chlorophenyl)-1-nitroethane and 1-(4-chlorophenyl)-2-nitropropane have not been done with $nNOS_{oxy}$.

These data underline the very similar behaviors of $iNOS_{oxy}$ (in the absence of BH_4 and L-Arg) and microsomal cytochromes P450 in the formation of iron(II)−nitrosoalkane complexes from reduction of nitroalkanes in the presence of dithionite. Many complexes of both heme proteins are

Table 2: Effect of L-Arginine, BH_4, and Three BH_4 Analogues on the Formation of the 448 nm Absorbing Complex Derived from i- and $nNOS_{oxy}$, Nitromethane, and Sodium Dithionite

	% 448 nm absorbing complex[a]						
	$-BH_4$	$+BH_4$[b]	+L-Arg (1 mM)	+L-Arg (1 mM) +BH4[b]	+(*6S*)-BH_4 (100 μM)	BH_2 (100 μM)	+6,7-diMe-TP (100 μM)
$iNOS_{oxy}$[c]	100	65 ± 7	41 ± 8	25 ± 6	53 ± 8	63 ± 7	66 ± 8
$nNOS_{oxy}$[d]	100	63 ± 8	34 ± 4	28 ± 4	41 ± 6	28 ± 4	84 ± 8

[a] Mean values ± SD from 3−6 experiments. [b] BH_4 concentrations used respectively for $iNOS_{oxy}$ and $nNOS_{oxy}$:**2** and 0.3 μM. [c] $iNOS_{oxy}$ (0.6 μM in 50 mM HEPES buffer, pH 7.4) was first incubated for 10 min at 20 °C without BH_4 or in the presence of BH_4, L-Arginine (1 mM), or BH_4 analogues (100 μM), before the addition of 20 mM sodium dithionite and 2 mM nitromethane, and scanning the absorption from 370 to 500 nm every minute for 10 min. [d] Similar experiments but in the presence of 0.45 μM $nNOS_{oxy}$.

formed even with hydrophobic and bulky nitrosoalkanes. This is not the case of heme proteins, such as hemoglobin, that have a more restricted access to the heme distal pocket (*30*).

Interestingly enough, stepwise addition of some hydrophobic nitroalkanes, 1-nitrohexane, and nitrocyclohexane, to $iNOS_{oxy}$ Fe(III) led to a difference spectrum with a peak around 390 nm and a trough at 422 nm, which is characteristic of a low-spin Fe(III) → high-spin Fe(III) transition. Such a difference spectrum is observed with L-arginine and corresponds to the binding of a substrate to a protein site close to the heme (*19*). These results indicate that the distal side of the heme of $iNOS_{oxy}$ is accessible to bulky nitroalkanes, which may undergo a two-electron reduction to corresponding nitrosoalkanes which are immediately trapped as strong iron(II) ligands.

Treatment of recombinant $iNOS_{oxy}$ not containing BH_4 with 5 M urea, followed by dialysis overnight, gives $iNOS_{oxy}$ mostly as a monomer (*43*). Reaction of 2 mM nitromethane with this monomer (0.8 μM) in the presence of excess dithionite also led to a 448 nm absorbing complex whose properties were identical to the corresponding complex of dimeric $iNOS_{oxy}$ (similar ϵ value and stability as a function of time; easy destruction with ferricyanide).

Reaction of Nitromethane with Full-Length iNOS. Recombinant full-length iNOS from *E. coli* containing the FAD, FMN, and heme prosthetic groups and purified in the absence of BH_4 and L-arginine (*38*) also reacted with nitromethane in the presence of dithionite with formation of a complex absorbing at 448 mn. This complex exhibited spectral characteristics (λ_{max} and ϵ) and chemical properties (stability toward CO and destruction by ferricyanide) almost identical to those of the dimeric and monomeric $iNOS_{oxy}$−Fe(II)−nitrosomethane complexes (data not shown).

Reaction of Nitroalkanes with the Oxygenase Domain of Neuronal NOS ($nNOS_{oxy}$) in the Presence of Dithionite. Recombinant $nNOS_{oxy}$ produced in *E. coli* and purified in the absence of BH_4 and L-Arg (*28*) reacted with nitroalkanes in the presence of dithionite in a manner very similar to $iNOS_{oxy}$. Complexes characterized by Soret peaks around 450 nm were also observed (Figure 4B); their properties (λ_{max}, ϵ values, stability in the presence of CO, and destruction by ferricyanide) were almost identical to those found for corresponding $iNOS_{oxy}$ complexes. The rates and extents of formation of the $nNOS_{oxy}$ complexes were lower than those of the $iNOS_{oxy}$ complexes, as shown in Table 1 and Figure 4B. For instance, formation of the complex derived from 2-nitropropane was complete after 7 min with $iNOS_{oxy}$, whereas only 50% of this complex was formed after 10 min in the case of $nNOS_{oxy}$ (compare panels A and B of Figure 4).

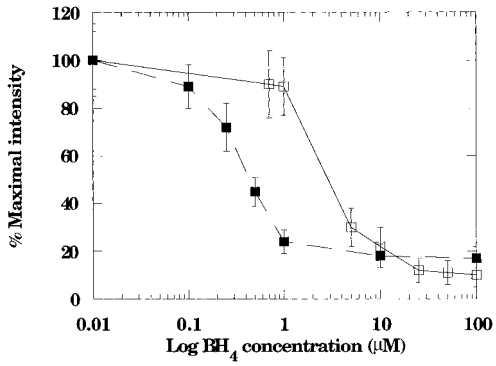

FIGURE 5: Effects of preincubation of $iNOS_{oxy}$ with BH_4 on its ability to form a CH_3NO_2-derived 448 nm absorbing complex. (□) $iNOS_{oxy}$, 0.6 μM, was preincubated with various concentrations of BH_4 for 10 min at 20 °C. Then the amount of 448 nm absorbing complex was measured by visible spectroscopy 10 min after addition of 2 mM CH_3NO_2 and 10 mM dithionite, at 20 °C. (■) Identical experiments performed with 0.35 μM $nNOS_{oxy}$. Mean values ± SD from 3−5 experiments.

Effects of the Presence of BH_4 on the Formation of i- and nNOS−Fe(II)−Nitrosoalkane Complexes. Preincubation of the recombinant iNOS oxygenase domain with BH_4 for 10 min at 20 °C led to a heme protein less capable to form 448 nm absorbing complexes upon reaction with nitromethane and dithionite. Preincubation of 0.5 μM $iNOS_{oxy}$ with 2 μM BH_4 decreased the amount of 448 nm absorbing complex to 65% of that observed with $iNOS_{oxy}$ not containing BH_4 (Table 2). Similar preincubations performed with increasing concentrations of BH_4 led to decreasing amounts of 448 nm absorbing complexes with an IC_{50} value about 4 μM (Figure 5). Preincubations with 1 mM L-arginine also decreased the amounts of complex formed under identical conditions (41%, Table 2), and it is noteworthy that preincubations of $iNOS_{oxy}$ with both 2 μM BH_4 and 1 mM L-arginine led to a low level of formation of 448 nm absorbing complex (Table 2).

Three BH_4 analogues, (*6S*)-BH_4, BH_2, and 6,7-dimethyl-5,6,7,8-tetrahydropterin, also acted as inhibitors of $iNOS_{oxy}$ complex formation; however, they were far less active, as preincubation of $iNOS_{oxy}$ with 100 μM of these analogues only led to a 40−50% inhibition (Table 2).

The formation of $iNOS_{oxy}$ complexes derived from 2-nitropropane and 1-nitrohexane was similarly inhibited by the preincubation of $iNOS_{oxy}$ in the presence of BH_4 (data not shown).

Similar effects of preincubation with BH_4, alone or in the presence of L-arginine, on nitrosoalkane complex formation were observed either with full-length iNOS or with $nNOS_{oxy}$. For instance, preincubation of recombinant full-length iNOS for 10 min at 20 °C with 100 μM BH_4 strongly decreased the appearance of a 448-nm peak after reaction of the enzyme

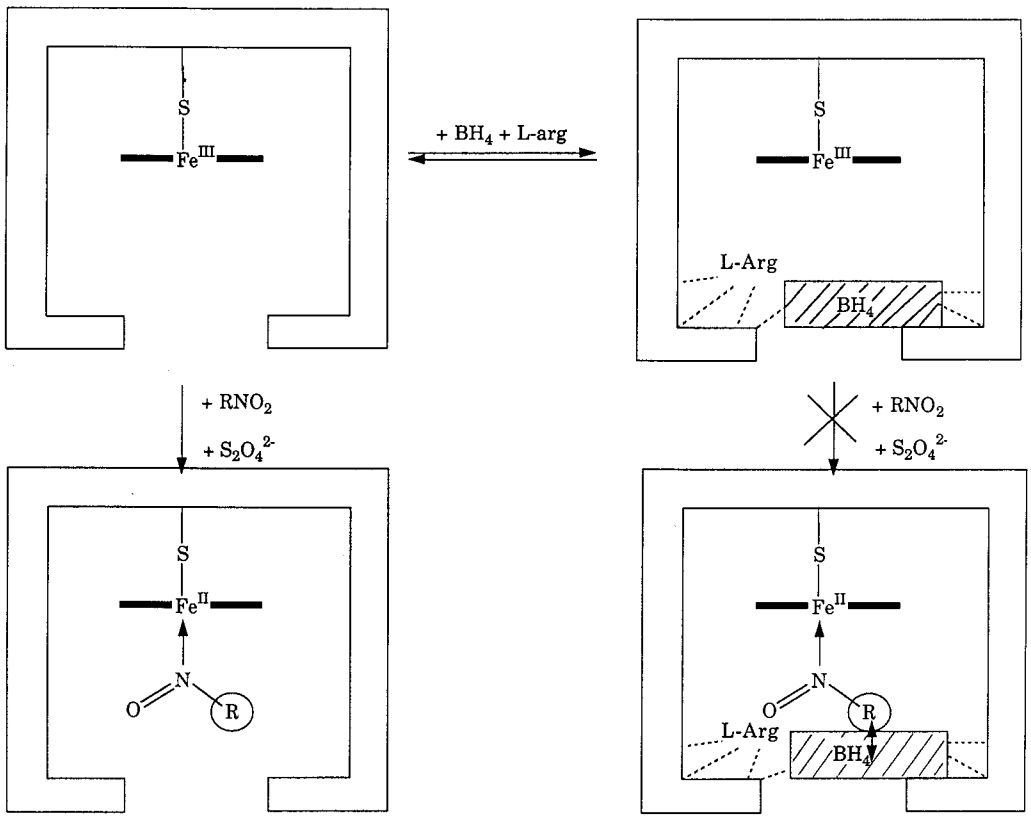

FIGURE 6: Schematic view of the active site of NOS, either in the absence of BH_4 and L-Arg ("P450"-like structure able to bind RNO ligands) or in the presence of BH_4 and L-Arg ("NOS"-type structure unable to bind RNO ligands).

with nitromethane and dithionite (30% of the intensity of the peak observed under identical conditions but without preincubation with BH_4). Moreover, Figure 5 shows that preincubation of 0.35 μM $nNOS_{oxy}$ with increasing concentrations of BH_4 leads to a marked decrease of the 448 nm absorbing complex formation, the IC_{50} found for BH_4 being in that case of 0.5 μM, a concentration not far from that of $nNOS_{oxy}$ used in this study. Preincubation in the presence of 0.3 μM BH_4 led to 63% complex formation, a further decrease to 28% complex formation being observed in the presence of both BH_4 (0.3 μM) and L-arginine (1 mM) (Table 2).

The three BH_4 analogues, BH_2, (*6S*)-BH_4, and 6,7-diMe-TP, were less active inhibitors of $nNOS_{oxy}$ complex formation when compared to BH_4 itself (28, 41 and 84%, respectively, compared to 18% for BH_4 for an inhibitor concentration of 100 μM; Table 2 and Figure 5). This order of inhibition efficiency, $BH_4 > BH_2 >$ (*6S*)-$BH_4 >$ 6,7-diMe-TP, follows the order of the binding constants of these pterin derivatives recently reported for nNOS (respective *K*'s of 0.23, 2.2, 19, and >1000 μM) (*45*). However, one must be careful with such a qualitative comparison, since the inhibition studies have been made on $nNOS_{oxy}$ and the measurement of the dissociation constants have been taken on full-length nNOS. Moreover, our comparison of the inhibitory effects of the pterin analogues is so far only based on one concentration (100 μM, Table 2).

These results suggest that catalytically active NOS containing its four prosthetic groups and L-arginine is unable to form 448 nm absorbing complexes upon reaction with nitroalkanes and dithionite. To verify this point, experiments were performed with purified neuronal NOS that was obtained from expression in yeast of rat brain NOS cDNA (see Materials and Methods and ref *40*) and contained its four prosthetic groups, FAD, FMN, heme, and BH_4.

Reaction of Nitroalkanes with Full-Length Neuronal NOS. Addition of 2 mM nitromethane and excess dithionite to 0.8 μM recombinant neuronal NOS that already contained its four natural prosthetic groups and L-arginine (1 mM) failed to lead to any significant difference spectrum. It is noteworthy that, under those conditions (2 mM nitromethane and presence of excess dithionite), full-length iNOS not containing BH_4 was completely converted to its iron(II)−nitrosomethane complex (data not shown).

DISCUSSION

In the absence of BH_4 and L-Arg, the oxygenase domains of iNOS and nNOS, as well as full-length iNOS, react with a variety of nitroalkanes in the presence of dithionite with formation of ferrous complexes characterized by a Soret peak around 450 nm. Those complexes exhibit chemical properties (stability toward CO and destruction by ferricyanide) that are identical to those previously described for iron(II)−nitrosoalkane complexes of several heme proteins such as hemoglobin, myoglobin, cytochromes P450, and prostaglandin H synthase, which have also been obtained by reduction of nitroalkanes in the presence of dithionite. Microsomal cytochromes P450 and NOSs without BH_4 exhibit an identical behavior for nitrosoalkane complex formation, as they seem to accept nitrosoalkanes of different size as distal iron(II) ligands, and as the spectral characteristics of those complexes are highly similar.

However, the formation of nitrosoalkane complexes of iNOS and nNOS is strongly inhibited by the presence of

BH_4. Actually, full-length nNOS, containing all its natural prosthetic groups, FAD, FMN, heme, and BH_4, and its substrate, L-arginine, appears unable to form nitrosoalkane complexes in the presence of nitroalkanes and dithionite. These results led us to propose that the heme distal active sites of iNOS− and nNOS−Fe(II) without BH_4 and L-arginine are largely accessible to even bulky nitrosoalkane ligands in a manner similar to microsomal cytochromes P450. The situation is completely different for iNOS and nNOS containing BH_4 and L-arginine whose heme appears unable to bind nitrosoalkanes as small as nitrosomethane. This effect of BH_4 is not due to an inhibition of NOS Fe(III) reduction by dithionite, as nNOS expressed in yeast and containing BH_4 and L-arginine exists under its Fe(II) form in the presence of dithionite (as shown by visible spectroscopy; data not shown). Moreover, there is no formation of nNOS−nitrosoalkane complexes in the presence of BH_4, dithionite, and CH_3NO_2 even after 20 min; this suggests that the presence of BH_4 does not simply decrease the rate of nNOS Fe(III) reduction by dithionite.

An explanation for the inhibitory effects of BH_4 on NOS−nitrosoalkane complex formation could be the strong binding of BH_4 to iNOS and nNOS in the distal part of the heme pocket and in close proximity of the heme, resulting in the locking of the active site (Figure 6). This concept of a solvent-exposed accessible distal part of the NOS heme pocket, only in the absence of BH_4 and L-Arg, is in agreement with several results previously reported on NOS Fe(III)−ligand complexes. Thus, dithiothreitol, a relatively bulky thiol, was found to readily bind to BH_4-free iNOS monomer, whereas this ligand is excluded in the presence of BH_4 or L-Arg (*24*, *42*, *46*). Moreover, very recent results about the formation of σ-aryl−iron complexes of recombinant iNOS, nNOS, and eNOS upon reaction with aryldiazenes showed that BH_4 directly binds above the heme pyrrole ring D and constricts that region. L-Arginine blocks access to the heme iron atom in all three NOS isoforms and nearly suppresses the phenyldiazene reaction (*27*).

However, it is noteworthy that the inhibitory effects of BH_4 alone on NOS Fe(III)−σ-aryl complex formation (*27*) are not as dramatic as on NOS Fe(II)−nitrosoalkane complex formation (this study). The reason for that is presently unclear; it could be related to differences between the size of the heme distal pocket, and its control by BH_4 binding, either in NOS Fe(III) (which is responsible for σ-aryl ligand binding) or in NOS Fe(II) (which binds nitrosoalkane ligands). In fact, in eNOS Fe(III) containing BH_4, the space for distal heme ligands was estimated to be $\sim 6.3 \times 6.7$ Å^2 from studies on rigid planar ligands, imidazoles, pyridines, and pyrimidines (*21*). The space for distal heme ligands in NOS Fe(II) could be smaller, as the binding of even very small ligands such as CO (*23*, *47*) and O_2 (*28*) appears to be affected by the presence of BH_4.

Our results indicate that the distal pocket of heme Fe(II) in BH_4-containing iNOS and nNOS cannot accommodate even the smallest nitrosoalkane ligand, CH_3NO. On the contrary, in the absence of BH_4, NOSs Fe(II) appear to be largely opened to much larger RNO ligands, with R = cyclohexyl or *p*-Cl−C_6H_4−$CH_2CH(CH_3)$, for instance (Figure 4), a behavior similar to that of microsomal cytochromes P450 (*34*). Comparison of the rates and extents of formation of nitrosoalkane complexes of $iNOS_{oxy}$ and $nNOS_{oxy}$ (Figure 4) suggests that the distal heme pocket of $iNOS_{oxy}$ without BH_4 is more accessible than that of $nNOS_{oxy}$; this is particularly clear for isopropyl-NO_2, which leads to a complete and relatively fast [0.32 nmol of complex (nmol of NOS)$^{-1}$ min^{-1}] formation of the $iNOS_{oxy}$ complex, but to a partial (50%) and slower formation of the corresponding complex with $nNOS_{oxy}$ [0.15 nmol of complex (nmol of NOS)$^{-1}$ min^{-1}].

This distal heme Fe(II) pocket of iNOS and nNOS seems to be closed upon binding of BH_4 and L-Arg, resulting in a restricted access for Fe(II) ligands except very small ones such as CO, NO, and O_2. Such effects of BH_4 in controlling the size of the distal heme pocket of NOS Fe(II) and in destabilizing NOS Fe(II) complexes (ref 28 and this work) could be due to a local steric phenomenon as shown in Figure 6 and as suggested in recent papers (*27*, *28*, *42*, *48*, *49*). However, one cannot presently exclude that it is related to a conformational effect due to the binding of BH_4 to a remote site of the protein. Anyway, it corresponds to a new role of biopterins in biological systems.

REFERENCES

1. Moncada, S., Palmer, R. M. J., and Higgs, E. A. (1991) *Pharmacol. Rev. 43*, 109−143.
2. Kerwin, J. F., and Heller, M. (1994) *Med. Res. Rev. 14*, 23−74.
3. Knowles, R. G., and Moncada, S. (1994) *Biochem. J. 298*, 249−258.
4. Förstermann, U., Closs, E. I., Pollock, J. S., Nakane, M., Schwartz, P., Gath, I., and Kleinert, H. (1994) *Hypertension 23*, 1121−1131.
5. Masters, B. S. S., McMillan, K., Sheta, E. A., Nishimura, J. S., Roman, L. J., and Martasek, P. (1996) *FASEB J. 10*, 552−558.
6. Bredt, D. S., Hwang, P. M., Glatt, C. E., Lowenstein, C., Reed, R. R., and Snyder, S. (1991) *Nature 351*, 714−718.
7. Su, Z., Blazing, M. A., Fan, D., and George, S. E. (1995) *J. Biol. Chem. 270*, 29117−29122.
8. Baek, K. J., Thiel, B. A., Lucas, S., and Stuehr, D. J. (1993) *J. Biol. Chem. 268*, 21120−21129.
9. Klatt, P., Schmidt, K., Lehner, D., Glatter, O., Bächinger, H. P., and Mayer, B. (1995) *EMBO J. 14*, 3687−3695.
10. Cho, H. J., Martin, E., Xie, Q. W., Sassa, S., and Nathan, C. (1995) *Proc. Natl. Acad. Sci. U.S.A. 92*, 11514−11518.
11. Tzeng, E., Billiar, T. R., Robbins, P. D., Loftus, M., and Stuehr, D. J. (1995) *Proc. Natl. Acad. Sci. U.S.A. 92*, 11771−11775.
12. Ghosh, D. K., and Stuehr, D. J. (1995) *Biochemistry 34*, 801−807.
13. Abu-Soud, H. M., Loftus, M., and Stuehr, D. J. (1995) *Biochemistry 34*, 11167−11175.
14. Klatt, P., Pfeiffer, S., List, B. M., Lehner, D., Glatter, O., Bächinger, H. P., Werner, E. R., Schmidt, K., and Mayer, B. (1996) *J. Biol. Chem. 271*, 7336−7342.
15. White, K. A., and Marletta, M. A. (1992) *Biochemistry 31*, 6627−6631.
16. Stuehr, D. J., and Ikeda-Saito, M. (1992) *J. Biol. Chem. 267*, 20547−20550.
17. McMillan, K., Bredt, D. S., Hirsch, D. J., Snyder, S. H., Clark, J. E., and Masters, B. S. S. (1992) *Proc. Natl. Acad. Sci. U.S.A. 89*, 11141−11145.
18. Sono, M., Stuehr, D. J., Ikeda-Saito, M., and Dawson, J. H. (1995) *J. Biol. Chem. 270*, 19943−19948.
19. McMillan, K., and Masters, B. S. S. (1993) *Biochemistry 32*, 9875−9880.
20. Matsuoka, A., Stuehr, D. J., Olson, J. S., Clark, P., and Ikeda-Saito, M. (1994) *J. Biol. Chem. 269*, 20335−20339.
21. Berka, V., Chen, P. F., and Tsai, A. L. (1996) *J. Biol. Chem. 271*, 33293− 33300.

22. Chabin, R. M., McCauley, E., Calaycay, J. R., Kelly, T. M., MacNaul, K. L., Wolfe, G. C., Hutchinson, N. I., Madhusudanaraju, S., Schmidt, J. A., Kozarich, J. W., and Wong, K. K. (1996) *Biochemistry 35*, 9567−9575.
23. Wang, J., Rousseau, D. L., Abu-Soud, H. M., and Stuehr, D. J. (1994) *Proc. Natl. Acad. Sci. U.S.A. 91*, 10512−10516.
24. Abu-Soud, H. M., Wang, J., Rousseau, D. L., Fukuto, J. M., Ignarro, L. J., and Stuehr, D. J. (1995) *J. Biol. Chem. 270*, 22997−23006.
25. Hurshman, A. R., and Marletta, M. A. (1995) *Biochemistry 34*, 5627− 5634.
26. Counts-Gerber, N., and Ortiz de Montellano, P. R. (1995) *J. Biol. Chem. 270*, 17791−17796.
27. Counts-Gerber, N., Rodriguez-Crespo, I., Nishida, C. R., and Ortiz de Montellano, P. R. (1997) *J. Biol. Chem. 272*, 6285−6290.
28. Abu-Soud, H. M., Gacchui, R., Raushel, F. M., and Stuehr, D. J. (1997) *J. Biol. Chem. 272*, 17349−17353.
29. Mansuy, D., Battioni, P., Chottard, J.-C., Riche, C., and Chiaroni, A. (1983) *J. Am. Chem. Soc. 105*, 455−463.
30. Mansuy, D., Chottard, J.-C., and Chottard, G. (1977) *Eur. J. Biochem. 76*, 617−623.
31. Mansuy, D., Gans, P., Chottard, J.-C., and Bartoli, J.-F. (1977) *Eur. J. Biochem. 76*, 607−615.
32. Mansuy, D., Battioni, P., Chottard, J.-C., and Lange, M. (1977) *J. Am. Chem. Soc. 99*, 6441−6443.
33. Mahy, J.-P., and Mansuy, D. (1991) *Biochemistry 30*, 4165−4172.
34. Mansuy, D., Battioni, P., and Battioni, J. P. (1989) *Eur. J. Biochem. 184*, 267−285.
35. Kornblum, N., and Wade, P. A. (1973) *J. Org. Chem. 38*, 1418−1420.
36. Gairaud, C. B., and Lappin, G. R. (1953) *J. Org. Chem. 18*, 1−3.
37. Schechter, H. S., Ley, D. E., and Roberson, E. B. (1956) *J. Am. Chem. Soc. 78*, 4984−4988.
38. Wu, C., Zhang, J., Abu-Soud, H., Ghosh, D. K., and Stuehr, D. J. (1996) *Biochem. Biophys. Res. Commun. 222*, 439−444.
39. Black, S. M., and Ortiz de Montellano, P. R. (1995) *DNA Cell Biol. 14*, 789−794.
40. Sari, M. A., Booker, S., Jaouen, M., Vadon, S., Boucher, J. L., Pompon, D., and Mansuy, D. (1996) *Biochemistry 35*, 7204−7213.
41. McMillan, K., and Masters, B. S. S. (1995) *Biochemistry 34*, 3686−3693.
42. Ghosh, D. K., Abu-Soud, H. M., and Stuehr, D. J. (1996) *Biochemistry 35*, 1444−1449.
43. Siddhanta, U., Wu, C., Abu-Soud, H. M., Zhang, J., Ghosh, D. K., and Stuehr, D. J. (1996) *J. Biol. Chem. 271*, 7309−7312.
44. Mansuy, D., Beaune, P., Cresteil, T., Bacot, C., Chottard, J.-C., and Gans, P. (1978) *Eur. J. Biochem. 86*, 573−579.
45. Klatt, P., Schmid, M., Leopold, E., Schmidt, K., Werner, E. R., and Mayer, B. (1994) *J. Biol. Chem. 269*, 13861−13866.
46. Gorren, A. C. F., List, B. M., Schrammel, A., Pitters, E., Hemmens, B., Werner, E. R., Schmidt, K., and Mayer, B. (1996) *Biochemistry 35*, 16735−16745.
47. Wang, J., Stuehr, D. J., and Rousseau, D. L. (1995) *Biochemistry 34*, 7080−7087.
48. Scheele, J. S., Kharitonov, V. G., Martasek, P., Roman, L. J., Sharma, V. S., Masters, B. S. S., and Magde, D. (1997) *J. Biol. Chem. 272*, 12523− 12528.
49. Wang, J., Stuehr, D. J., and Rousseau, D. L. (1997) *Biochemistry 36*, 4595−4606.

BI972297S